

## Isothermal phase transition and elastic energy dissipation in $\text{YBa}_2\text{Cu}_3\text{O}_{6+x}$

E. Bonetti, E. G. Campari, M. D'Astuto, and M. Marangolo

*Dipartimento di Fisica, Università di Bologna and Istituto Nazionale per la Fisica Della Materia,  
viale Berti-Pichat 6/2, I-40127 Bologna, Italy*

(Received 8 August 1994)

Neutron-diffraction data collected under vacuum at 680 and 695 K have been compared with elastic energy dissipation and dynamic Young's modulus measurements in  $\text{YBa}_2\text{Cu}_3\text{O}_{6+x}$ . The orthorhombic to tetragonal phase transition has been observed in isothermal conditions. The data suggest that a phonon softening occurs at the oxygen disordering, which, in these experimental conditions, precedes the phase transition. The elastic energy dissipation presents a peak above room temperature. Its origin and behavior are discussed in terms of an oxygen atom repopulation model, with activation energy depending on the orthorhombic strain and oxygen ordering in the basal plane.

### INTRODUCTION

It is nowadays well established that the structure<sup>1</sup> and electronic properties of  $\text{YBa}_2\text{Cu}_3\text{O}_{6+x}$  depend on the oxygen stoichiometry, at a fixed cation ratio. The critical superconducting temperature is accordingly a sensitive function of deviations from the exact stoichiometry.<sup>2</sup> The system presents a high oxygen mobility, in particular of the atoms in the  $(\frac{1}{2}00)$  and  $(0\frac{1}{2}0)$  positions of what is usually called the basal plane. In and out diffusion predominantly occurs in that plane<sup>3</sup> and strongly depends on temperature and pressure.

As a consequence, the  $\text{YBa}_2\text{Cu}_3\text{O}_{6+x}$  presents various oxygen-deficient phases, each stable in a specific temperature, pressure, and oxygen content range.<sup>4,5</sup> These phases are characterized by different ordering degrees of the oxygen sublattice sites. Observations by electron microscopy and neutron-diffraction techniques have indicated that the so-called orthorhombic II phase is the most stable among the different substoichiometric ones.<sup>6,7</sup> It consists of alternatively full and empty chains along the  $b$  axis.

Neutron-diffraction studies at ambient pressure<sup>1,8</sup> have shown that at high oxygen content and low temperatures the oxygen atoms are ordered along the  $b$  axis. The equilibrium phase is orthorhombic. With increasing temperature, the oxygen ions begin to disorder. Finally, for each  $x$  value, a temperature is reached where, in equilibrium conditions, the oxygen ions are evenly distributed over the  $(\frac{1}{2}00)$  and  $(0\frac{1}{2}0)$  sites, and the lattice develops tetragonal symmetry.

Measurements of elastic energy dissipation (internal friction) have been, in recent years, extensively applied to the study of short-range-order oxygen dynamics as a function of stoichiometry as well as for the study of the structural transformations linked to the oxygen in and out diffusion. This technique consists of putting into vibration a sample, usually bar shaped, and measuring its resonance frequency and vibration amplitude as it dies away. The technique is very sensitive to detect atomic motion between different lattice sites or interstitial posi-

tions. In  $\text{YBa}_2\text{Cu}_3\text{O}_{6+x}$  its usefulness stems from the fact that an elastic strain can easily modify the  $(\frac{1}{2}00)$  and  $(0\frac{1}{2}0)$  occupation degree, the oxygen atoms being the most mobile species in this compound. Consequently, strong anelastic effects associated to short-range-order dynamics can be expected. Experimental measurements performed by different research groups,<sup>9-15</sup> following the measurements by Berry,<sup>16</sup> have confirmed that in the temperature range where appreciable oxygen mobility is expected, strong relaxational damping maxima can be detected.

There is an increasing amount of experimental data demonstrating that the system exhibits two thermally activated peaks with activation energy of 1-1.5 eV.<sup>17-19</sup> One of them is typical of oxygen-rich specimens:  $x \approx 0.9$ , while the other has maximum intensity for  $x \approx 0.5$ . Their activation energy, relaxation time, and a clear, even if not simple, dependence of their intensity on the oxygen stoichiometry, suggest that they are due to the oxygen mobility. A number of models, based on internal friction data, have been proposed to explain the peak origin. Unfortunately, the data do not seem to be clear enough to unambiguously attribute the peaks to some specific mechanism.

In this paper, we present internal friction and dynamic modulus data obtained on  $\text{YBa}_2\text{Cu}_3\text{O}_{6+x}$  samples of different stoichiometry. Some of the data refer to samples prepared with  $x > 0.9$  and kept under vacuum at (constant) temperatures high enough to allow an oxygen outflow. In these measurements the sample is in thermal equilibrium but out of equilibrium in regard to the oxygen content, and we measure the kinetics with which the equilibrium is reached. These data are correlated with the results of neutron diffraction obtained in the same experimental conditions. The Rietveld refinement of the neutron data during the equilibrium approach provided us with a number of changing structural parameters. We will explain in the following how these isothermal measurements, together with the usual measurements as a function of temperature, can help our understanding of the detailed mechanism of the above-mentioned internal friction peaks. Furthermore, we present the first experi-

mental evidences of an orthorhombic oxygen disordered state.

### EXPERIMENTAL

$\text{YBa}_2\text{Cu}_3\text{O}_{6+x}$  samples were produced by the standard solid-state reaction technique: Yttrium, barium and copper oxides reacted, while kept at 1220 K in a flowing oxygen atmosphere for 8 h, and were subsequently annealed at 770 K for 8 h. The reacted powders were pressed in pellets, annealed in oxygen, and ground several times.<sup>20</sup> This procedure gives nearly stoichiometric samples, with  $x > 0.9$  and up to  $x = 0.95$ . All internal friction measurements were performed on sintered bars produced with this technique, while powders used for the neutron measurements were obtained from ground bars. Typical specimen dimensions were  $20 \times 5 \times 1 \text{ mm}^3$ . The oxygen content of as-cast specimens was measured by iodometric titration, and the results were found in satisfactory agreement with those obtained by neutron diffraction. Small amounts of impurity phase are present in the samples and are probably responsible for the differences of the oxygen values measured with the two methods.

Neutron-powder-diffraction data were collected at 680 and 695 K with the multidetector powder diffractometer G4.1 at the Orphée Reactor facility (Leon Brillouin Laboratory, CEA-CNRS, Saclay, France) using a wavelength  $\lambda = 0.243 \text{ nm}$ . The collected data, belonging to the angular range  $10^\circ < 2\theta < 90^\circ$  were analyzed with the Rietveld refinement program Fullprof, which allows the simultaneous refinement of more phases.<sup>21</sup> An orthorhombic and tetragonal phase spectra, respectively, are reported in Figs. 1(a) and 1(b). Their successive refinement also in-

cluded two impurity phases: CuO and  $\text{Y}_2\text{BaCuO}_5$ . Each diffraction spectra was collected in slightly less than 1000 s in vacuum ( $p < 0.1 \text{ Pa}$ ). In such a time interval, a small amount of oxygen outflows the sample, so that it is possible to regard each spectrum as referring to a constant oxygen content. This hypothesis is well supported by the data (see, for example, Fig. 6 in the discussion).

Dynamic Young's modulus (modulus in short) and internal friction measurements were performed by the vibrating-reed technique,<sup>22</sup> with electrostatic drive and frequency modulation detection of the flexural vibration of cantilever mounted specimens, in the  $(10^2 - 10^4)\text{-Hz}$  range in a vacuum ( $p < 1 \text{ Pa}$ ) or in the  $(10^0 - 10^2)\text{-Hz}$  range with a torsion pendulum in air.<sup>22</sup> Measurements were performed during heating runs at 2–3 K/min up to 850 K for the  $(10^2 - 10^4)\text{-Hz}$  range and up to 700 K for the lower frequency range. Thermogravimetric measurements performed using a Netzsch thermobalance on dummy samples and neutron-diffraction measurements allowed us to monitor the oxygen outflow under vacuum in our experimental conditions. An oxygen outflow becomes easily measurable on a laboratory time scale at temperatures above 650 K under vacuum. On the other hand, no appreciable oxygen content variation is measured during heating in air up to the temperatures used with the torsion pendulum.

A series of isotherms at selected temperatures ( $680 \text{ K} < T < 780 \text{ K}$ ) under the same vacuum condition described above was performed for times up to  $3 \times 10^5 \text{ s}$ . Isotherms at temperatures higher than 780 K will cause the sample to turn into the tetragonal phase before or at the beginning of the isotherm because of the increasingly fast oxygen outflow; temperatures below 680 K would require days of measurements, with experimental condition stability problems. In both neutron-diffraction and internal friction isotherm tests the temperature was raised starting from room temperature at about 15–20 K/min and subsequently kept stable within  $\pm 1 \text{ K}$  of the chosen temperature.

### DISCUSSION

#### Internal friction peaks

When measuring as a function of temperature the internal friction and dynamic Young's modulus of an  $\text{YBa}_2\text{Cu}_3\text{O}_{6+x}$  bar with oxygen content equal to 6.9 or greater, a  $Q^{-1}$  peak, whose intensity is usually between 0.01 and 0.04, is seen around 680 K (1 kHz). It will be referred to as peak  $P_{01}$ . A modulus relaxation is observed in accordance with it; see Figs. 2(a) and 2(b). The peak is larger than a simple Debye peak<sup>14</sup> of

$$Q^{-1} = \Delta \frac{\omega\tau}{1 + \omega^2\tau^2} \quad (1)$$

and asymmetric.  $\omega$  is the sample resonance angular frequency and  $\tau$  the relaxation time. The peak asymmetry is due to the fast oxygen outflow, which occurs in a vacuum above 650 K, resulting in the oxygen disordering in the basal plane and in the transformation from orthorhombic to tetragonal phase. The process is accompanied by a fall

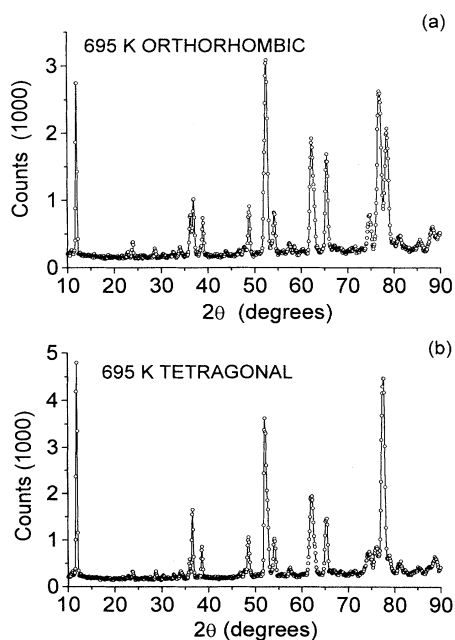


FIG. 1. (a) Neutron-diffraction data collected at  $T = 695 \text{ K}$ . This spectrum was subsequently refined as orthorhombic. (b) Same specimen and temperature as before but  $3 \times 10^4 \text{ s}$  later. This spectrum was refined as tetragonal.

of the internal friction peak and by a downward modulus cusp. In measurements performed in air at a few Hz frequency, without oxygen outflow, the peak is located at lower temperature, is still an enlarged Debye peak, is symmetric, and there is no cusp in the modulus trend.

In subsequent runs in the same experimental conditions, a peak whose position is about 90–100 K lower in temperature than  $P_{01}$ , is observed; see Fig. 3. It is again larger than a simple Debye peak, and its strength is a function of the oxygen content in the sample, with a maximum around 6.5.<sup>18</sup> It will be referred to as peak  $P_{02}$ .

These two peaks, which have been observed by other groups,<sup>18,19</sup> are thermally activated; that is  $\tau = \tau_0 \exp(H/kT)$ , where  $k$  is the Boltzmann constant,  $T$  the temperature,  $\tau_0$  the relaxation time, and  $H$  the activation energy of the process (that is the height of the potential barrier seen by the oxygen atoms, in the hypothesis that the peak occurs because of the oxygen jumping in the basal plane). Their activation energies were measured by several authors.<sup>11,15,17–19,23</sup> The most accurate result was published by Cost and Stanley,<sup>23</sup> who gave an activa-

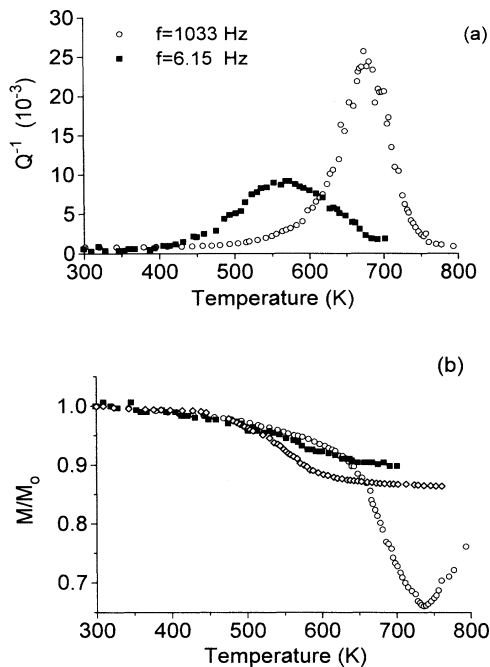


FIG. 2. (a) Elastic energy dissipation as a function of time for specimens with  $x > 0.9$ . The low-frequency sample (full squares) was measured with a torsional pendulum in air and the high-frequency one (open circles) with a vibrating-reed apparatus under vacuum conditions. Data were acquired during heating, with temperature raising at 2–3 K/min. The frequency reported in the figure was measured at room temperature at the beginning of the test. (b) Dynamic modulus corresponding to the curves in (a). Also reported is the modulus curve of a second run under vacuum on the sample whose internal friction is shown in Fig. 3. The statistical uncertainties of the data are smaller than the size of the symbols.

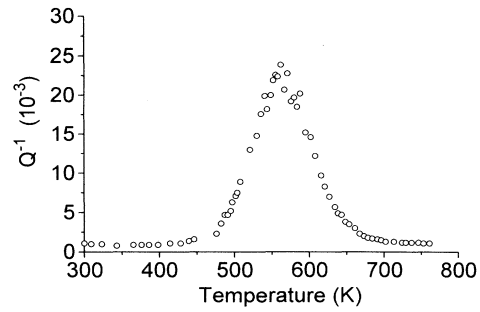


FIG. 3. Elastic energy dissipation measured in second run under vacuum with raising temperature. Note the different position of the peak with respect to Fig. 1(a). Resonance frequency at room temperature 1612 Hz.

tion energy of  $(1.120 \pm 0.015)$  eV. This result was obtained by joining data of the mechanical aftereffect with those of internal friction (independent data of several experimental groups) to span a frequency range of more than 11 orders of magnitude.

A Debye peak, Eq. (1), has its maximum at  $\omega\tau = 1$  and, if thermally activated, occurs at temperatures changing with frequency. A plot of the logarithm of  $\tau$  taken at the maximum vs  $1/kT$  for a series of measures with different sample resonance frequency, will be a straight line whose slope is  $H$ . Then, the wider the frequency range, the better the measure of  $H$ . Cost and Stanley also analyzed the peak width in terms of a distribution of relaxation times, suggesting that local inhomogeneity in the system in nonstoichiometric conditions causes the peak broadening. Unfortunately, some of the data used for the activation energy calculation comes from samples of unknown stoichiometry or submitted to an anneal under vacuum (oxygen outflow) before the measurement. All data were considered to belong to one peak only (reasonably  $P_{02}$ ), but this is probably not true. We measured an activation energy of  $(1.54 \pm 0.09)$  eV for  $P_{01}$  and  $(1.3 \pm 0.1)$  eV for  $P_{02}$ . We cannot discount that our results are affected by some error. In fact, as will be better explained further on during the discussion, in our experimental conditions stoichiometric effects are possible, which bring about mistakes in the peak position evaluation.

Nevertheless, the peak activation energies and their dependence on the oxygen content<sup>22</sup> suggested from the beginning that their origin could be due to some kind of oxygen motion in the lattice. As revealed by neutron- and x-ray-diffraction measurements,<sup>8,24</sup> the oxygen atoms in positions  $(\frac{1}{2}00)$  and  $(0\frac{1}{2}0)$  of the unit cell are by far the most mobile of all atomic species in this compound. This restricted the models to certain mechanisms, only involving the motion of oxygen atoms between these positions. We will consider three models, which are to us the most promising to explain the experimental observations; see Fig. 4.

(a) The motion of the oxygen basal-plane atoms occurring at the twin boundaries, which are present in the orthorhombic phases.<sup>6,17,18</sup> This model comes from the observation that the orthorhombic phase is rich in twins,

that is, boundaries between crystals with  $a$  and  $b$  axes interchanged. In these boundaries the oxygen mobility would be particularly high and originate the elastic energy dissipation. Twins are observed in the orthorhombic II phase also, while they cannot be present in the tetragonal phase, where  $a=b$ . The peak height would depend on the sample preparation, which determines the twin density, and on the oxygen content.

(b) The dipole reorientation model, where the dipole or

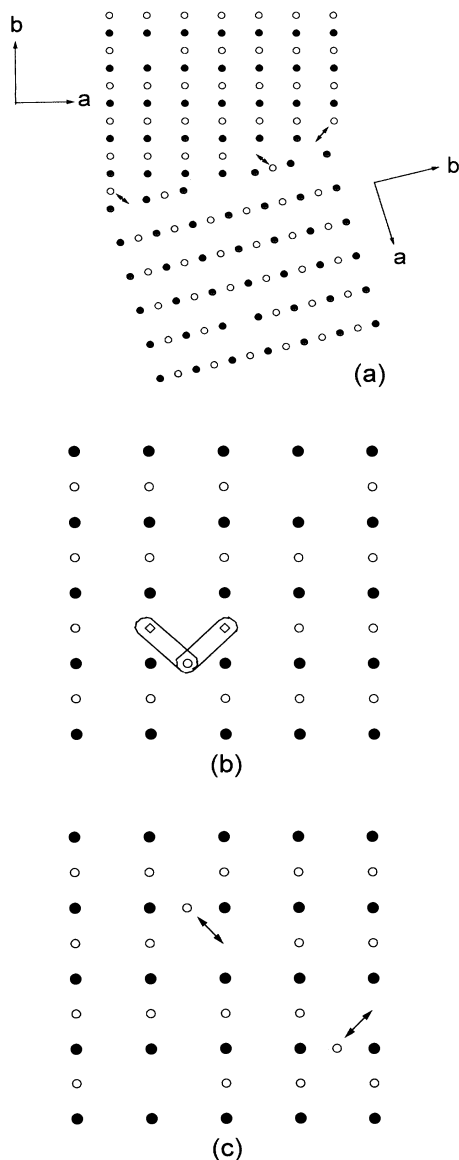


FIG. 4.  $\text{YBa}_2\text{Cu}_3\text{O}_{6+x}$  basal plane with oxygen atoms (open circles) and copper atoms (full circles). (a) A twin boundary. The arrows suggest possible oxygen atomic jumps in correspondence to the boundary. (b) Dipole model. The two possible dipole orientations are sketched in this figure. (c) Repopulation model. The oxygen atom jumps along the  $a$  and  $b$  axes are indicated by the arrow.

elastic lattice deformation is made of an oxygen in position  $(\frac{1}{2}00)$  and a lattice vacancy in position  $(0\frac{1}{2}0)$ .<sup>23</sup> Such a dipole represents a defect with monoclinic symmetry in an orthorhombic lattice and thus could cause an elastic energy dissipation through reorientation between the  $[110]$  and  $[-110]$  directions under the action of an applied stress. In this model the peak should only be present in the orthorhombic phases because in a tetragonal lattice the two oxygen positions are equivalent, and an oxygen atom in  $(\frac{1}{2}00)$  or in  $(0\frac{1}{2}0)$  would no longer represent an elastic deformation of the same kind. The peak intensity would depend on the dipole number, and an oxygen disordering in the orthorhombic phase should be accompanied by an internal friction increase, since a disordering would mean an increased dipole number.

(c) Site repopulation model.<sup>17,18,23</sup> In this model the oxygen atoms, under the action of the applied stress, which slightly modifies the energy levels of the  $(\frac{1}{2}00)$  and  $(0\frac{1}{2}0)$  lattice positions, change their relative concentration along the  $a$  and  $b$  axes. The peak is present in all crystal phases, and its intensity depends on the oxygen content and relaxation rate. The main difference between (b) and (c) is that two atomic jumps are needed for the reorientation of an elastic dipole, while a single jump from  $(0\frac{1}{2}0)$  to  $(\frac{1}{2}00)$  or vice versa is the elemental action in the repopulation scheme.

#### Order-disorder transformation

In the usual tests with raising temperature, both temperature and oxygen content vary. In order to reduce the number of contemporary changing parameters, we decided to study the system behavior in isothermal conditions. Figures 5(a) and 5(b) show the internal friction of two isotherms, at the temperatures of 680 and 730 K, while Figs. 6 and 7 show the oxygen content and the basal-plane axis lengths for  $T=680$  and 695 K as deduced from the neutron data refinement. The modulus trend, reported in Fig. 8 at different temperatures as a function of the logarithm of time, is as classically predicted for a second-order phase transition, that is, with a downward cusp. The behavior, with oxygen replacing temperature, is as follows (Ref. 22, Chaps. 16 and 25):

$$M = \frac{M_0}{1 + c/|T - T_c|} \quad (2)$$

with  $c$  constant and  $M_0$  the limit value for  $T \rightarrow \infty$ .

It is found from observation of the oxygen content as a function of time, as reported in Fig. 6, that a logarithmic time scale corresponds quite well to a linear oxygen change. Thus, the choice of a logarithmic scale in Fig. 8 is the most appropriate, since at constant temperature the oxygen concentration  $x$  can be the driving parameter for the transformations undergone by the system. The curves of Fig. 8 can indeed be rescaled with temperature to be superimposed. This confirms that the different time position of the cusp in isotherms at different temperatures is due to the same process occurring at different rates.

In regard to which process underlines the modulus

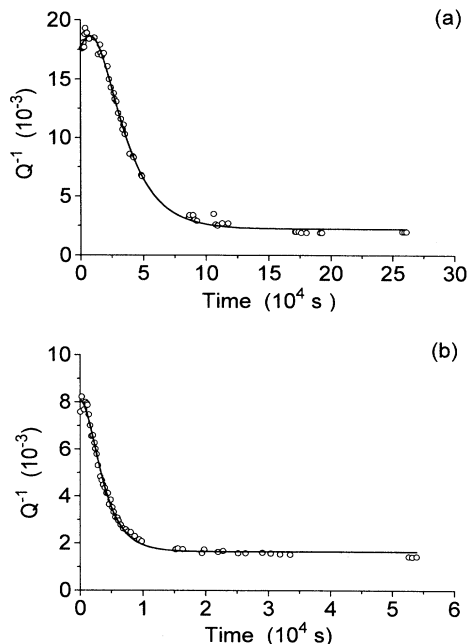


FIG. 5. Internal friction of two different samples, produced with  $x > 0.9$  as a function of time during an isothermal test at 680 K (a) and 730 K (b). The full lines represent a best fit of the data using Eq. (8). Note the different time scales at which the decreasing trend is accomplished.

minimum, the most obvious idea is that it is an effect of the orthorhombic-to-tetragonal phase transformation on the elastic constants. Unfortunately, this does not seem to be the case. The neutron refinements on two samples at 680 and 695 K done within the same vacuum conditions under which we collected the modulus data show that there is no agreement as regards the cusp and the phase-transition time position. Assuming that the orthorhombic-to-tetragonal transformation occurs when the axes difference is  $(b - a) = 0$ , the symmetry change at

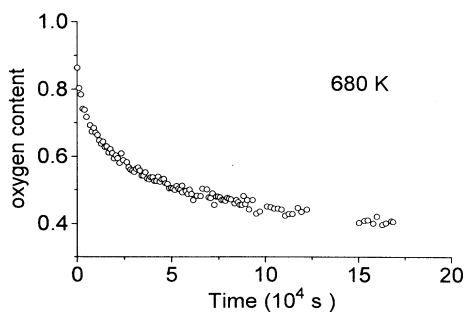


FIG. 6. Oxygen content  $x$  in the basal plane as a function of time as deduced from a Rietveld refinement for the isotherm at  $T = 680$  K. The exponential-like trend suggested the choice of the logarithmic scale in Fig. 8. The experimental uncertainties are not bigger than the size of the symbol.

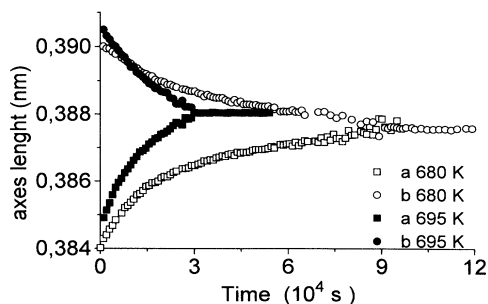


FIG. 7. Length of the  $a$  and  $b$  unit-cell axes of  $\text{YBa}_2\text{Cu}_3\text{O}_{6+x}$  as a function of time as deduced from Rietveld refinement of the isotherms at  $T = 680$  and 695 K. The system was refined with an orthorhombic phase until when  $a = b$  within experimental uncertainties; then a tetragonal phase was used.

$T = 680$  K surely happens between  $8.5 \times 10^4$  and  $9 \times 10^4$  s, while the modulus cusp is located between  $2.7 \times 10^4$  and  $2.8 \times 10^4$  s. A similar difference, rescaled for the temperature, is observed at 695 K.

Then, which phenomenon does the modulus softening correspond to? We believe it is the effect of the oxygen disordering between the  $(0\frac{1}{2}0)$  and  $(\frac{1}{2}00)$  positions. What might happen is that, at a given oxygen content and fixed temperature, the system free-energy minimum corresponds to a disordered state. This hypothesis is supported by the neutron-diffraction data refinement. As can be seen in Fig. 9, the refinement sequence suggests an equal occupation of the two basal plane sites at times corresponding to the modulus cusp. The time at which the oxygen occupancy  $n(a)$  along the  $a$  axis and  $n(b)$  along the  $b$  axis becomes equal was assumed to correspond to an oxygen disordered state. We believe the data need confirmation, especially for the 680-K isotherm, where they are rather scattered mainly because of the little temperature fluctuations and the instrument peak-shape resolution. In fact, while the axis length could be well

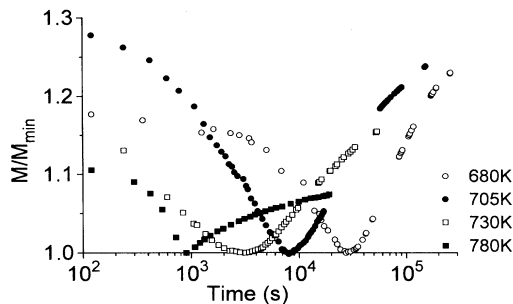


FIG. 8. Dynamic modulus behavior of a series of isotherms at different temperatures as a function of the logarithm of time. All curves refer to samples measured under vacuum and were normalized to their minimum value, to better show how the cusp position shifts at lower times when the isothermal temperature increases from 680 to 780 K.

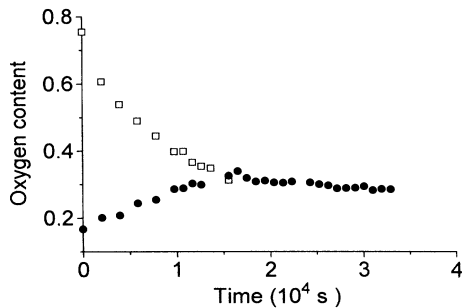


FIG. 9. Oxygen occupancy along the  $a$  (full circle) and  $b$  (open squares) axes  $[(\frac{1}{2}00)$  and  $(0\frac{1}{2}0)$  positions] as deduced from Rietveld refinement of the isotherm at  $T=695$  K. The occupancy becomes equal after approximately  $1.3 \times 10^4$  s.

refined, there are sometimes convergence problems for other parameters such as the sites occupancy. Nevertheless, even the 680-K data should be considered in agreement with the disordering hypothesis.

In previous works on neutron diffraction as a function of oxygen content,<sup>8,26</sup> the oxygen disordering was reported to occur at the phase transition, that is, the tetragonal phase is always disordered, while the orthorhombic phase is always ordered. But while samples were kept at high temperatures and low pressures to reduce the oxygen content, they were successively brought back to room temperature, where the neutron-diffraction test was performed. A cooling of 400 K or more can well cause an oxygen reordering of an orthorhombic disordered sample and thus explain the different results. Furthermore, it must be recalled that during the isotherm the system is out of equilibrium, at least in regard to the oxygen content.

In Fig. 10 the occupancy  $n(a)$  and  $n(b)$  along the basal-plane axes is reported as a function of the oxygen content at  $T=695$  K. The  $a$  and  $b$  axis occupancy becomes equal without any apparent discontinuity. The occupancy order parameter  $n(b)-n(a)$  results to be a linear function of the orthorhombic strain, as shown in Fig. 11 and reported elsewhere,<sup>8</sup> but the line does not

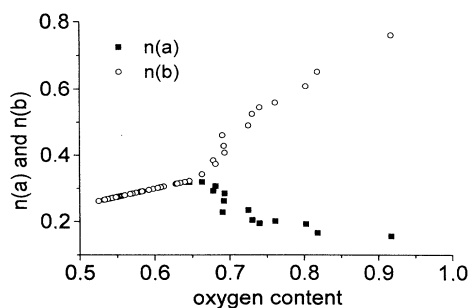


FIG. 10. Oxygen occupancy along the  $a$  and  $b$  axes as a function of the oxygen content for the  $T=695$  K isotherm.

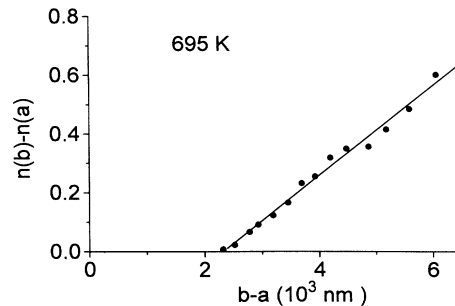


FIG. 11. Site occupancy order parameter  $[n(b)-n(a)]$  as a function of the orthorhombic strain  $(b-a)$  as deduced from Rietveld refinement of the isotherm at  $T=695$  K.

pass through the origin, since phase and disordering transformation does not occur at the same time. In Fig. 12 the cell volume is shown at 680 and 695 K as a function of time. Again, only the expected volume increase is seen, without any discontinuity. This supports the idea that in this temperature range the orthorhombic-to-tetragonal transformation, as well as the oxygen disordering, is a second-order process.

A mathematical description of the order-disorder transformation can be given employing the Bragg-Williams long-distance order theory (Refs. 27 and 28, Chap. 4). With reference to the  $\text{YBa}_2\text{Cu}_3\text{O}_{6+x}$  basal plane, one may define right and wrong "objects," where oxygen atoms along the  $b$  axis and oxygen vacancies along the  $a$  axis are defined as "right;" oxygen vacancies along the  $b$  axis and oxygen atoms along the  $a$  axis are defined as "wrong." If  $R$  is the "right object" number and  $W$  the "wrong object" number referring to the actual stoichiometry, then  $R+W=2 \times N$ , with  $N$  the cell number. With this definition, we avoid counting as wrong the vacancy along the  $b$  axis present in a full ordered specimen with  $x < 1$ . A long-distance order parameter is defined by

$$S = \frac{R - W}{2xN}, \quad (3)$$

so that  $S=1$  in a completely ordered state, regardless to

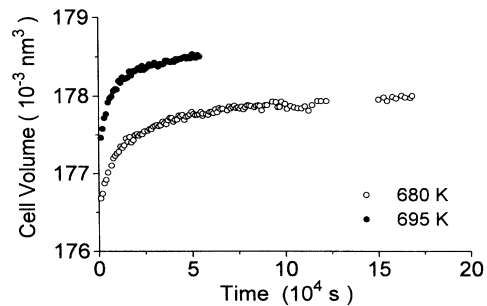


FIG. 12. Cell volume as deduced from Rietveld refinement of the isotherms at  $T=695$  K (full circles) and  $T=680$  K (open circles).

the system stoichiometry.

Suppose the energy required to produce a pair of wrong objects in the state  $R, W$  is  $\Phi(R, W)$ . The configurational entropy associated with the state  $R, W$  is  $S_{cf} = k(N \ln N - R \ln R - W \ln W)$ . Thus, the change  $\Delta S_{cf}$  associated with  $\Delta W$  (wrong object number variation; here an oxygen atom moving from  $b$  to  $a$  axis) is

$$\Delta S_{cf} = -k(\Delta R \ln R + \Delta W \ln W) = 2k \ln(R/W). \quad (4)$$

Since in thermal equilibrium the change  $\Delta F$  in the free energy associated with  $\Delta W$  must vanish ( $\Delta W \ll W$ ), neglecting thermal entropy changes, one can readily find the equilibrium values by writing

$$\begin{aligned} \Delta F = 0 &= \Phi(R, W) - T \Delta S_{cf} \\ &= \Phi(R, W) - 2kT \ln(R/W) \end{aligned} \quad (5)$$

or

$$\frac{R}{W} = \exp \left[ \frac{\Phi(R, W)}{2kT} \right]. \quad (6)$$

Finally, with the given definitions of  $R$ ,  $W$ ,  $n(a)$ , and  $n(b)$ , it results that  $R/W = n(b)/n(a)$ .

In the framework of the Bragg-Williams theory, a simple linear relationship between  $\Phi(R, W)$  and  $S$  is introduced as an assumption:  $\Phi(R, W) = \Phi_0 S$ , where  $\Phi_0$  is the energy required to produce two wrong objects in the completely ordered lattice ( $S = 1$ ). This is equivalent to a nearest-neighbor interaction model.<sup>33</sup> An implicit equation for  $r = \Phi_0 S / 4kT$  is obtained:

$$S = \tanh(\Phi_0 S / 4kT). \quad (7)$$

Nontrivial solutions, corresponding to an ordered state, can be obtained for  $r > r$  (critical). At each temperature a critical  $\Phi_{0c}$  value exists below which the system is in a disordered state. The higher the temperature in isothermal conditions, the higher the critical  $\Phi_{0c}$  value. In our dynamical measurements  $\Phi(R, W)$  changes with the orthorhombic deformation, which decreases because of the oxygen outflow. An essential point is that, due to the entropic term, a disordered state with  $(0\frac{1}{2}0)$  and  $(\frac{1}{2}00)$  sites differing in energy is possible.

#### Internal friction at fixed temperature

Let us turn now to the elastic energy dissipation in isothermal conditions. The internal friction, which, at about 700 K, has values close to the  $P_{01}$  peak maximum at kHz frequency, after a transient, decreases to the background value. A good fit to the data (full line in Fig. 5) was obtained from Eq. (1) with a time varying activation energy  $H$ . With  $H = 1.5$  eV,  $\tau_0 \cong 10^{-15} \text{ s}^{-1}$  and using the appropriate  $\omega$  value, a 10%  $H$  shift is enough to reduce the  $P_{01}$  peak strength from its maximum to the background. For this reason the activation energy time dependence was taken as linear:  $H(t) = H_{\max} - at$ , with  $H_{\max}$  the activation energy for the stoichiometric oxygen content and  $a$  a constant. Equation (1) becomes

$$Q^{-1} = \Delta \frac{A \exp(-t/\tau)}{1 + A^2 \exp(-2t/\tau)} \quad (8)$$

with  $\tau = kT/\alpha$ ,  $A = \omega \tau_0 \exp(H_{\max}/kT)$ . This function, after a transient time depending on temperature, reduces to a simpler exponential decay:  $Q^{-1} \cong \Delta A \exp(-t/\tau)$ . We, therefore, suggest that as an effect of the oxygen outflow, peak  $P_{01}$  shifts in position. The temperature shift corresponding to an energy difference of 0.2 eV (the difference between  $P_{01}$  and  $P_{02}$ ) can be deduced by the ratio  $H_1/H_2 = T_2/T_1$  and is about 90 K at kHz frequency, just the difference observed for our samples. Then, we suggest that in isothermal conditions the internal friction decrease is an effect of a position changing peak. What causes the shift is a change in the activation energy, which corresponds to the barrier height seen from the jumping oxygen atoms. The activation energy has a maximum when  $x = 1$ , like the orthorhombic strain, and progressively decreases moving towards the orthorhombic II phase and the tetragonal phase.<sup>10</sup>

Apart from our isothermal data, the  $P_{01}$  peak shift is reported by other authors<sup>19</sup> or can be deduced by published data<sup>18</sup> referring to measures as a function of temperature. In the first case, the authors claim that the shift is only present in  $\text{YBa}_2\text{Cu}_3\text{O}_{6+x}$  with aluminum partially substituting copper, while in the second the authors concentrate on the varying strength of the peak with oxygen content. Unluckily, in these papers the oxygen content was not measured, so it is difficult to say what really was the thermodynamic state of the samples. To make things more complicated, the peak strength also is depending on the oxygen content, while the system has a tendency towards phase separation. There are observations of phase inhomogeneity or the contemporary presence of orthorhombic I and II phases in samples with various oxygen content,<sup>22,29,30</sup> and calculations that predict possible phase separations with  $x$  values up to  $x = 0.94$ .<sup>31</sup> This explains why in certain cases<sup>17,32,19</sup>  $P_{01}$  and  $P_{02}$  are both present for the same oxygen content:  $P_{01}$  is the peak of the jumping oxygen in the orthorhombic I phase and  $P_{02}$  refers to the same kind of effect in the orthorhombic II phase. These two phases correspond to different potential barriers for the atoms and, as a consequence, should give peaks that are always distinct in position.

In a fully oxygenated specimen the atoms arrange in a pure orthorhombic I phase and only  $P_{01}$  should be present. As oxygen outflows, the peak shifts towards lower temperatures (at fixed frequency). Recalling that the peak is caused by the oxygen atoms, its strength should decrease as the oxygen outflows, while some authors claim it should increase.<sup>18,19</sup> It is possible that a dependence on the preparation condition and on the annealing time has some importance determining the peak strength. Furthermore, following the hypothesis of a change in the peak activation energy and a repopulation model, a change in the peak height is also deduced. The oxygen atoms in the basal plane are one of two potential energy minima. Their  $(\frac{1}{2}00)$  and  $(0\frac{1}{2}0)$  occupancy  $n(a)$  and  $n(b)$  are expected to follow Eq. (6), so that at fixed temperature

$$\frac{n(a)}{n(b)} = \exp(-\Delta E/kT) \quad (9)$$

with  $\Delta E$ , the two-site energy difference corresponds to  $\Phi(R, W)/2$ . Recalling Eq. (7), the energy site difference corresponding to the disordering can be simulated. It is 0.11 eV at  $T=680$  K and 0.12 eV at  $T=695$  K. These values can be compared with those calculated by Chen and Wu<sup>10</sup> on samples annealed in air at temperatures of 680 K or more that have different oxygen contents.

The effect of a little sinusoidal deformation on the energy of each level will be to periodically increase and then decrease their energy by an amount  $\sigma$  (small with respect

to the original energy value). This energy variation will cause a change in the population of each level. If  $n(a)$  is the equilibrium population along the  $a$  axis before the application of a stress, the new population will be given by

$$n'(a) = \frac{x \exp[(2\sigma + \Delta E)/kT]}{1 + \exp[(2\sigma + \Delta E)/kT]} \quad (10)$$

The difference  $n'(a) - n(a)$  is the level repopulation. Now, a decrease in activation energy and in the difference  $\Delta E$  between levels will give a new expression like (10). The difference between the two cases represents the effect of an energy level change on the stress-induced repopulation. This effect can be written as

$$\Delta(\text{repopulation}) = x \left[ \frac{\exp(\Delta E/kT)}{1 + \exp(\Delta E/kT)} - \frac{\exp[(2\sigma + \Delta E)/kT]}{1 + \exp[(2\sigma + \Delta E)/kT]} + \frac{\exp[(2\sigma + \Delta E')/kT]}{1 + \exp[(2\sigma + \Delta E)/kT]} - \frac{\exp(\Delta E'/kT)}{1 + \exp(\Delta E'/kT)} \right] \quad (11)$$

where  $\Delta E'$  is the new energy difference. Equation (11) reduces to

$$\Delta = x \{ [\exp(\Delta E/kT) - \exp(\Delta E'/kT)] \times [1 - \exp(2\sigma/kT)] \} \quad (12)$$

when  $1 \gg \exp(\Delta E/kT)$ , which is satisfied (with  $\Delta E < 0$ ) if  $|\Delta E| \geq 0.2$  eV. From Eq. (11) it is possible to evaluate how a reduced energy level difference causes an increased repopulation between the two sites as an effect of an applied stress. The intensity of the phenomenon depends on  $\sigma$ , but reasonable values can easily bring about a repopulation variation of two times or even more. As a result of this we expect a peak-intensity increase as the peak shifts towards lower temperatures.

With decreasing  $x$ , the system enters the orthorhombic II phase existence range. Then  $P_{02}$  appears and rises in intensity, with a maximum around  $x=0.5$ , where that phase is stoichiometric. At even lower oxygen concentrations  $P_{02}$  decreases. Peak  $P_{02}$  should also shift with oxygen content, which is not clearly seen in the experiments. What might happen is that an oxygen outflow in these conditions triggers a change in the relative proportions of the various phases present in the sample so that the orthorhombic II phase decreases in volume keeping nearly constant  $a$  and  $b$  axis values. In Ref. 18 a peak corresponding well to  $P_{02}$  is measured in a sample with  $x$  estimated to be equal to 0.3, which is tetragonal, at least macroscopically. The peak is rather feeble immediately after quenching down to room temperature from 990 K and increases without appreciable shift after thermal treatments. This could well be an oxygen ordering and particularly the formation of further orthorhombic II phases during the slow cooling from high temperature.

No clear observations of the system in a pure tetragonal phase are available because of the tendency to the formation of orthorhombic microdomains in macroscopically tetragonal samples. Even samples with overall tetrago-

nal symmetry and oxygen content below 6.5 exhibit a temperature range where the basal-plane oxygen atoms are not completely disordered but are aligned in small chains, and orthorhombic domains exist. There is evidence of a peak around 500 K at 1 kHz frequency, which could be due to the tetragonal phase, even if it is uncertain whether the peak is thermally activated or not. The latter case would strongly support the hypothesis that the peak corresponds to some kind of structural transformation.<sup>18</sup> (We also obtained similar results on a sample annealed 2.5 h at 1000 K in flowing argon.) It must be underlined that these specimens, treated at high temperature to reduce the oxygen content, also present a partial chemical decomposition (formation of  $Y_2BaCuO_5$ ), which complicates the data analysis. Finally, there are claims<sup>13</sup> that the peak occurring in the tetragonal phase has a really low activation energy of 0.11 eV, being located below 100 K at about 1 kHz frequency.

## CONCLUSIONS

The most reasonable mechanism originating the peaks existing in  $YBa_2Cu_3O_{6+x}$  above room temperature seems to be the repopulation process. The main reason to exclude a twin mechanism is because an internal friction peak can be measured in conditions where twins are absent because the system is made of such small oxygen-atom-ordered domains that the concept of twins lose meaning. Nevertheless, it must be said that a direct measure assuring that  $P_{01}$  or  $P_{02}$  exists in twin free samples has never been done, at least to our knowledge. At the same time, the complete absence of any internal friction increase during the isothermal tests, described above in the discussion, seems to be a major inconvenience for the dipole model proposed by Cost and Stanely.<sup>23</sup> In spite of the oxygen outflow, as oxygen disorders between the  $a$  and  $b$  axes, the dipole number increases. Since the peak intensity is directly dependent on the dipole number, and



we are measuring at or near the peak maximum, an internal friction increase strong enough to be easily detected should be present. On the contrary, only a monotonous decrease (Fig. 5) is seen.

What is left is then the repopulation mechanism. We also suggest that the peak activation energy changes with the orthorhombic strain and with the kind of order of the oxygen atoms in the basal plane.  $P_{01}$  as shown in Fig. 2(a) is the peak due to the repopulation in an oxygen-rich orthorhombic I specimen;  $P_{02}$  (Fig. 3) is caused by the same process in the orthorhombic II phase, corresponding to a smaller activation energy of about 0.2 eV. The peak intensity depends on several factors: oxygen content, energy difference between ( $\frac{1}{2}00$ ) and ( $0\frac{1}{2}0$ ) sites, and phase volume. We are trying at the moment to theoretically predict the peak intensity as a function of all parameters.

Finally, the phonon softening attributed to the orthorhombic to tetragonal phase transition, observed for the first time by Tallon, Schuitema, and Tapp<sup>9</sup> working at 40-kHz frequency and successively on our samples at 1

kHz,<sup>33</sup> is an effect of the oxygen atom disordering in the basal plane. This explanation is suggested by the comparison of modulus and neutron-diffraction measurements. Under vacuum, a temperature range exists where the kinetics of the oxygen outflow and phase transformation are such that the  $\text{YBa}_2\text{Cu}_3\text{O}_{6+x}$  system turns into an oxygen-disordered orthorhombic phase. The modulus downward cusp, predicted for a second-order phase transition, corresponds to the oxygen-disordering and not to the lattice-symmetry transformation.

#### ACKNOWLEDGMENTS

The authors would like to acknowledge the Istituto di Metallurgia of Bologna University for providing the samples and, in particular, A. Zingaro for their preparation and characterization and J. C. Rodriguez-Carvajal for providing the refinement program and for assisting during the neutron data collection. We also acknowledge the Laboratoire Leon Brillouin and the U.E. for funding us during our stay in Saclay.

- <sup>1</sup>J. D. Jorgensen, B. W. Veal, A. P. Paulikas, L. J. Nowicki, G. W. Crabtree, H. Claus, and W. K. Kwok, *Phys. Rev. B* **41**, 1863 (1990).
- <sup>2</sup>H. Maletta, *Physica C* **169**, 371 (1990).
- <sup>3</sup>S. I. Bredikhin, G. A. Emel'chenko, V. S. Schechtman, A. A. Zhokhov, S. Carter, R. J. Chater, J. A. Kilner, and B. C. H. Steele, *Physica C* **179**, 286 (1991).
- <sup>4</sup>G. Ceder, M. Asta, and D. de Fontaine, *Physica C* **177**, 106 (1990).
- <sup>5</sup>N. H. Andersen, B. Lebech, and H. F. Poulsen, *J. Less Common Metals* **164&165**, 124 (1990).
- <sup>6</sup>G. van Tendeloo, D. Broddin, H. W. Zandbergen, and S. Amelinckx, *Physica C* **167**, 627 (1990).
- <sup>7</sup>R. A. Hadfield, P. Schleger, H. Casalta, N. H. Handersen, H. F. Poulsen, M. Zimmermann, J. R. Schneider, M. T. Hutchings, D. A. Keen, R. Liang, P. Dosanjh, and W. H. Hardy, *Physica C* (to be published).
- <sup>8</sup>J. D. Jorgensen, M. A. Beno, D. G. Hinks, L. Soderholm, K. J. Volin, R. L. Hitterman, J. D. Grace, I. K. Shuller, C. U. Segre, K. Zhang, and M. S. Kleefish, *Phys. Rev. B* **36**, 3608 (1987).
- <sup>9</sup>J. L. Tallon, A. H. Schuitema, and N. E. Tapp, *Appl. Phys. Lett.* **52**, 507 (1988).
- <sup>10</sup>X. Xie, T. Chen, and Z. Wu, *Phys. Rev. B* **40**, 4549 (1989).
- <sup>11</sup>J. X. Zhang, G. M. Lin, Z. C. Lin, K. F. Liang, P. C. W. Fung, and G. G. Siu, *J. Phys. Condens. Matter* **1**, 6939 (1989).
- <sup>12</sup>E. Bonetti, E. G. Campari, A. Casagrande, and S. Mantovani, in *High Temperature Superconductivity*, edited by C. Ferdeghini and A. S. Siri (World Scientific, Singapore, 1990), p. 223.
- <sup>13</sup>G. Cannelli, R. Cantelli, F. Cordero, M. Ferretti, and F. Trequattrini, *Solid State Commun.* **77**, 429 (1991).
- <sup>14</sup>J. R. Cost and J. T. Stanley, *J. Mater. Res.* **6**, 232 (1991).
- <sup>15</sup>J. Woiregard, A. Riviere, P. Gadaud, and P. Tal, *Europhys. Lett.* **17**, 601 (1992).
- <sup>16</sup>B. Berry, *Bull. Am. Phys. Soc.* **33**, 512 (1988).
- <sup>17</sup>E. Bonetti, E. G. Campari, and S. Mantovani, *Physica C* **196**, 7 (1992).
- <sup>18</sup>G. Cannelli, R. Cantelli, F. Cordero, F. Trequattrini, S. Ferraro, and M. Ferretti, *Solid State Commun.* **80**, 715 (1991).
- <sup>19</sup>X. M. Xie and T. G. Chen, *Supercond. Sci. Technol.* **5**, 290 (1992).
- <sup>20</sup>E. Bonetti, E. G. Campari, G. P. Cammarota, A. Casagrande, and G. Centi, in *Second European Conference on Advanced Materials and Processes*, *Advanced Materials and Processes*, Book 531 (The Institute of Metals, London, 1991), p. 75.
- <sup>21</sup>J. Rodríguez Carvajal, *Physica B* **192**, 55 (1993).
- <sup>22</sup>A. S. Nowick and B. S. Berry, *Anelastic Relaxation in Crystalline Solids* (Academic, New York, 1972).
- <sup>23</sup>J. R. Cost and J. T. Stanley, *Mater. Sci. Forum* **119-121**, 623 (1993).
- <sup>24</sup>A. W. Hewat, J. J. Capponi, C. Chaillout, M. Marezio, and E. A. Hewat, *Solid State Commun.* **64**, 301 (1987).
- <sup>25</sup>*Internal Friction in Solids: Proceedings of the Summer School on Internal Friction in Solids, Krakov, 1984*, edited by S. Gorczyca and L. B. Magalas (Wydawnictwo AGH, Krakov, 1984).
- <sup>26</sup>P. G. Radaelli, C. U. Segre, D. H. Hinks, and J. D. Jorgensen, *Phys. Rev. B* **45**, 4923 (1992).
- <sup>27</sup>W. L. Bragg and E. J. Williams, *Proc. R. Soc. London, Ser. A* **145**, 699 (1934).
- <sup>28</sup>A. J. Dekker, *Solid State Physics* (MacMillan, London, 1962).
- <sup>29</sup>V. Plakhty, B. Kviatkovsky, A. Stratilatov, Y. Chernenkov, P. Burlet, J. Y. Henry, C. Marin, E. Ressouche, J. Schweizer, F. Yakou, E. Elkaim, and J. P. Lauriat, *Physica C* (to be published).
- <sup>30</sup>T. Zeiske, R. Sonntag, D. Hohlwein, N. H. Andersen, and T. Wolf, *Nature (London)* **353**, 542 (1991).
- <sup>31</sup>A. A. Gorbatsevich, Y. V. Kopaev, and I. V. Takatly, *Physica C* **223**, 95 (1994).
- <sup>32</sup>E. Bonetti, E. G. Campari, G. P. Cammarota, A. Casagrande, and S. Mantovani, *J. Less-Common Met.* **164&165**, 231 (1990).
- <sup>33</sup>E. Bonetti, E. G. Campari, T. Manfredini, and S. Mantovani, *Physica C* **179**, 381 (1991).